Mechanisms of late restriction induced by an endogenous retrovirus

Frederick Arnaud, Pablo R Murcia, Massimo Palmarini

JOURNAL OF VIROLOGY, Oct. 2007, p. 11441–11451 Vol. 81, No. 20
0022-538X/07/$08.00+0 doi:10.1128/JVI.01214-07

Mechanisms of Late Restriction Induced by an Endogenous Retrovirus[▽]

Frederick Arnaud, Pablo R. Murcia, and Massimo Palmarini*

Institute of Comparative Medicine, University of Glasgow Veterinary School, 464 Bearsden Road, Glasgow, Scotland

Received 3 June 2007/Accepted 1 August 2007

The host has developed during evolution a variety of "restriction factors" to fight retroviral infections. We investigated the mechanisms of a unique viral block acting at late stages of the retrovirus replication cycle. The sheep genome is colonized by several copies of endogenous retroviruses, known as enJSRVs, which are highly related to the oncogenic jaagsiekte sheep retrovirus (JSRV). enJS56A1, one of the enJSRV proviruses, can act as a restriction factor by blocking viral particles release of the exogenous JSRV. We show that in the absence of enJS56A1 expression, the JSRV Gag (the retroviral internal structural polyprotein) targets initially the pericentriolar region, in a dynein and microtubule-dependent fashion, and then colocalizes with the recycling endosomes. Indeed, by inhibiting the endocytosis and trafficking of recycling endosomes we hampered JSRV exit from the cell. Using a variety of approaches, we show that enJS56A1 and JSRV Gag interact soon after synthesis and before pericentriolar/recycling endosome targeting of the latter. The transdominant enJS56A1 induces intracellular Gag accumulation in microaggregates that colocalize with the aggresome marker GFP-250 but develop into bona fide aggresomes only when the proteasomal machinery is inhibited. The data argue that dominant-negative proteins can modify the overall structure of Gag multimers/viral particles hampering the interaction of the latter with the cellular trafficking machinery.

The host has developed a variety of mechanisms during evolution, beside conventional innate and acquired immunity, to fight retroviral infections (4). For example, the constitutive expression of several proteins, known as "restriction factors," such as Fv-1, Fv-4, TRIM5α, and APOBEC3G, inhibit retrovirus replication (2, 3, 5, 15, 18, 31, 39, 41, 48). Some of these proteins are cellular in origin while others, such as Fv-1 and Fv-4, derive from inherited endogenous retroviruses (ERVs) (6).

ERVs derive from ancient retroviral infections of the germ line of the host and are transmitted vertically to subsequent generations according to Mendelian rules, due to the stable integration of the retroviral genome (known as "provirus") into the genomic DNA of the host cell. One of the biological roles attributed to ERVs is the protection of the host against incoming pathogenic retrovirus infections (3, 5, 28).

Studies on restriction factors, both of cellular and viral origin, are important to devise new antiretroviral strategies and to further understand viral replication and virus-host coevolution. The majority of restriction factors discovered thus far act at the early stages of the retrovirus replication cycle such as at entry or around reverse transcription and therefore are effective on newly infected cells.

We have described a potentially unique mechanism of viral interference between a transdominant ERV of sheep (enJS56A1) and the exogenous pathogenic jaagsiekte sheep retrovirus (JSRV) (23). JSRV is the causative agent of ovine pulmonary adenocarcinoma, one of the main viral diseases of sheep and a large animal model for lung cancer (25, 29).

The sheep genome is colonized by several copies of ERVs highly related to JSRV and known as enJSRVs (10, 26, 27). enJSRVs are abundantly expressed in the reproductive tract of the ewe and are essential in the early development of the sheep conceptus (11, 12, 26–28). In addition, enJSRVs can interfere with JSRV replication (23, 28, 40). enJS56A1, one of the enJSRV proviruses, can block viral particle release by the exogenous JSRV by a unique mechanism of viral interference acting at a late step of the replication cycle. For simplicity, we refer to this viral block as "JLR" for JSRV late restriction (23, 45).

The transdominant enJS56A1 has intact open reading frames for all its major structural genes, including *gag* that encodes the polyprotein forming the retroviral capsid. We have shown that enJS56A1 expression in vitro results in the production of abundant intracellular Gag that assembles (at least partially) considering that intracellular viral particles are visible by electron microscopy (23, 27). enJSRVs/JSRV are Betaretroviruses such as Mason-Pfizer monkey virus (M-PMV) and mouse mammary tumor virus that assemble in the cytoplasm ("type B-D assembly"), while human immunodeficiency virus (HIV) and other retroviruses assemble at the cell membrane ("type C assembly") (17, 38, 42).

enJS56A1 cannot release viral particles in the supernatant of transfected cells, and this defect is transdominant over the related exogenous JSRV (24). The main determinant of JLR is a tryptophan residue (W21) in position 21 of the matrix (MA) domain of the enJS56A1 polyprotein Gag, which substitutes an arginine (R21) conserved in JSRV and in all known betaretroviral MAs.

We have recently demonstrated that enJSRV-20, another provirus in the sheep genome, displays W21 in Gag and in-

* Corresponding author. Mailing address: Institute of Comparative Medicine, University of Glasgow Veterinary School, 464 Bearsden Road, Glasgow, G61 1QH Scotland, United Kingdom. Phone: 44-(0)141-3302541. Fax: 44-(0)141-3302271. E-mail: m.palmarini@vet.gla.ac.uk.

▽ Published ahead of print on 15 August 2007.

duces JLR. Most interestingly, both enJS56A1 and enJSRV-20 have acquired the R21W substitution in Gag in two temporally distinct events during evolution of the domestic sheep (*Ovis aries*), suggesting that this trait has been positively selected (Arnaud et al., unpublished).

JLR depends on Gag-Gag interactions between JSRV and enJS56A1 (24). Expression of enJS56A1 Gag appears to alter the pattern of localization of the JSRV Gag staining within cells, resulting in a reduction of the number of cells showing Gag accumulation at the microtubule organization center (MTOC)/pericentriolar region (24).

In the present study, we dissected JSRV and enJS56A1 Gag kinetics and intracellular trafficking in order to better understand this unique mechanism of viral restriction. Our results indicate that in the absence of enJS56A1 expression, JSRV Gag targets initially the MTOC in a dynein- and microtubule-dependent fashion and then colocalizes with the pericentriolar recycling endosomes, which are used to reach the cell membrane and exit from the cell. Using a variety of approaches, we show that enJS56A1 interacts with JSRV Gag soon after synthesis and before MTOC/recycling endosome targeting of the latter. The transdominant enJS56A1 determines intracellular Gag accumulation in microaggregates that will develop in an aggresome only when the proteasomal machinery is inhibited. The data argue that mutations in the matrix domain can induce overall alterations in Gag conformation, resulting in defective particles and/or multimers that cannot interact with the cell trafficking machinery but accumulate in the cytoplasm and are degraded by the proteasome.

MATERIALS AND METHODS

Plasmids. Plasmids pCMV4JS21, pCMV2en56A1, JSRVHA-MA, enJS56A1 FLAG-MA, and JSRV-G2A have been described previously (23, 24, 27, 29). pCMV4JS21 and pCMV2en56A1 express the full-length $JSRV_{21}$ molecular clone and the endogenous provirus enJS56A1. JSRVHA-MA and enJS56A1FLAG-MA express JSRV and enJS56A1 with Gag tagged, respectively, with the Ha and FLAG epitopes in the matrix domain. JSRV-G2A expresses the full-length JSRV but contains a G2A mutation in Gag, resulting in a defect of myristoylation. JSRV-G2AR21W and enJS56A1-G2A were obtained by site-directed mutagenesis, using QuikChange (Stratagene) as suggested by the manufacturer. EΔ95/295 is a green fluorescent protein (GFP)-tagged Eps15 dominant-negative mutant that inhibits clathrin-dependent endocytosis. DIIIΔ2 derives from Eps15 but does not inhibit endocytosis and is used as a negative control for EΔ95/295. Both plasmids were kindly provided by A. Benmerah (1). GFP-250 is an aggresome marker and was a gift from E. S. Sztul (14). p50-GFP expresses the dynamitin subunit of the dynactin complex fused with GFP and blocks specifically the dynein-dependent transport. p50-GFP was kindly provided by Richard Vallee (13).

Cell cultures, transfections, and viral preparations. 293T, HeLa, and COS cells were cultured in Dulbecco modified Eagle medium supplemented with 10% fetal bovine serum at 37°C, 5% CO_2, and 95% humidity. For Western blot analysis, virus was produced by transient transfection of 293T cells using the Calphos mammalian transfection kit (Clontech) according to the manufacturer's instructions. Cell supernatants were collected at 24 h posttransfection, and viral particles were concentrated by ultracentrifugation. For analysis of intracellular proteins, cells were lysed by standard techniques as already described (23). In order to inhibit cell endocytosis and dynein-dependent transport, Eps dominant-negative/control mutants and p50-GFP, respectively, were cotransfected with pCMV4JS21 expression plasmid. The cellular proteasomal machinery was blocked by treating cells with 100 μM lactacystin (Sigma; from a stock solution solubilized in ethanol [EtOH]) for 12 h.

siRNA experiments. Small interfering RNA (siRNA) analysis was performed by using double-stranded validated Stealth RNA (Invitrogen) oligonucleotides against Rab11a and Rab11b. Cells were incubated in OptiMEM (Invitrogen) with 30 nM concentrations of each siRNA duplex and Lipofectamine 2000 transfection reagent (Invitrogen) according to the manufacturer's instructions for 24 h. BLOCK-iT fluorescent oligonucleotides (Invitrogen) was used as a control of transfection efficiency and 60 nM concentrations of a scrambled Stealth RNA as negative control. After 24 h, 2 μg of JSRV expressing plasmid was transfected with Rab11 or control siRNAs for 4 h, medium was replaced, and supernatants were collected 3, 6, and 12 h after transfection.

Western blotting. Sodium dodecyl sulfate-polyacrylamide gel electrophoresis (SDS-PAGE) and Western blotting were performed as previously described on concentrated viral particles and cell lysates (50 μg of protein extracts) (29). Gag proteins were detected with a rabbit polyclonal sera against the JSRV major capsid protein (CA) (24). Rab11a (Abcam) and γ-tubulin (Sigma) proteins were detected with specific rabbit polyclonal antibodies. Membranes were exposed to the appropriate peroxidase-conjugated secondary antibodies and further developed by chemiluminescence using ECL Plus (Amersham). When necessary, Western blots were quantified by scanning membranes and measuring chemifluorescence in a Molecular Dynamics Storm 840 imaging system using ImageQuant TL software (Molecular Dynamics). Experiments (from transfections to Western blotting) were performed independently at least three times and are presented as the mean value for each sample (± the standard error).

Confocal microscopy. Most experiments were performed both in HeLa and COS cells. Both cell lines were plated onto two well-chambered glass slides (Lab-Tek; Nalge Nunc International) and transfected with Lipofectamine (Invitrogen) according to the manufacturer's instructions. In some experiments, cells were treated 24 h posttransfection with the microtubule inhibitor nocodazole (Sigma) at 50 μM for 4 h or with the proteasome inhibitor lactacystin (Sigma) at 100 μM for 6 to 12 h solubilized in dimethyl sulfoxide or EtOH, respectively. Cells were washed with phosphate-buffered saline (PBS) and fixed with 3% formaldehyde for 15 min. After fixation, cells were processed essentially as already described (23, 38). Gag proteins were detected using a rabbit antiserum toward JSRV MA (p23) preadsorbed with HeLa cell extracts to minimize background. Gag proteins differentially tagged with either the hemagglutinin (HA) or FLAG epitopes were detected with mouse monoclonal anti-HA (Covance) antibodies or rabbit polyclonal FLAG (Sigma) antiserum. Mouse monoclonal antibodies to γ-tubulin (Abcam), Rab11a (Abcam), calnexin (Abcam), TGN38 (Abcam), CD63 (Abcam), EEA1 (Abcam), and Dcp1a (gift of J. Lykke-Andersen) were used as markers for, respectively, the centrosome, recycling endosomes, endoplasmic reticulum, trans-Golgi bodies, late endosomes, early endosomes, and processing bodies. Lyso Tracker Red DND-99 (Molecular Probes), Dcp1a-GFP (a gift from G. Hannon) and GFP-G3BP (a gift from J. Tazi) were used as markers for, respectively, lysosomes, processing bodies, and stress granules. Polyubiquitinylated residues were stained with the mouse monoclonal antibody Fk1 (Affinity Research Products). An anti-vimentin-labeled Cy3 antibody (Molecular Probes) was used to detect the vimentin network. Goat anti-mouse and anti-rabbit immunoglobulin G conjugated, respectively, with Alexa Fluor 594 and Alexa Fluor 488 (Molecular Probes) were used as secondary antibodies. Slides were mounted with medium containing DAPI (4′,6′-diamidino-2-phenylindole; Vectashield, Vector Laboratories) and analyzed with a Leica TCS SP2 confocal microscope. Single sections from confocal optical sections along the z axis were analyzed.

Time course experiments with JSRV, enJS56A1, and JSRV-G2A were performed as follows. Cells were transfected with Lipofectamine and fixed after 3 h (experimental time zero) and then after 2, 4, 6, 8, 12, and 24 h. Immunofluorescence was performed as described above.

Transferrin uptake experiments were performed 24 h after transfection with the appropriate plasmids as described in Results. Cells were serum starved for 1 h and then incubated for 30 min in serum-free medium containing 60 μg of transferrin/ml conjugated with Alexa Fluor 568. Cells were then washed and fixed in 3% formaldehyde as described above.

RESULTS

Kinetics of JSRV/enJS56A1 Gag trafficking. The first question we wanted to address was at what point of the replication cycle enJS56A1 blocks JSRV. We initially assessed the kinetics of Gag localization and intracellular trafficking in JSRV- and enJS56A1-expressing cells. In previous studies, we have shown that cells expressing JSRV display three different patterns of Gag staining as revealed by confocal microscopy using an antiserum toward JSRV MA: uniformly "diffused," "dispersed" in discrete intracytoplasmic dots, or prevalently "concentrated" in a perinuclear region (23, 24). Intermediate pheno-

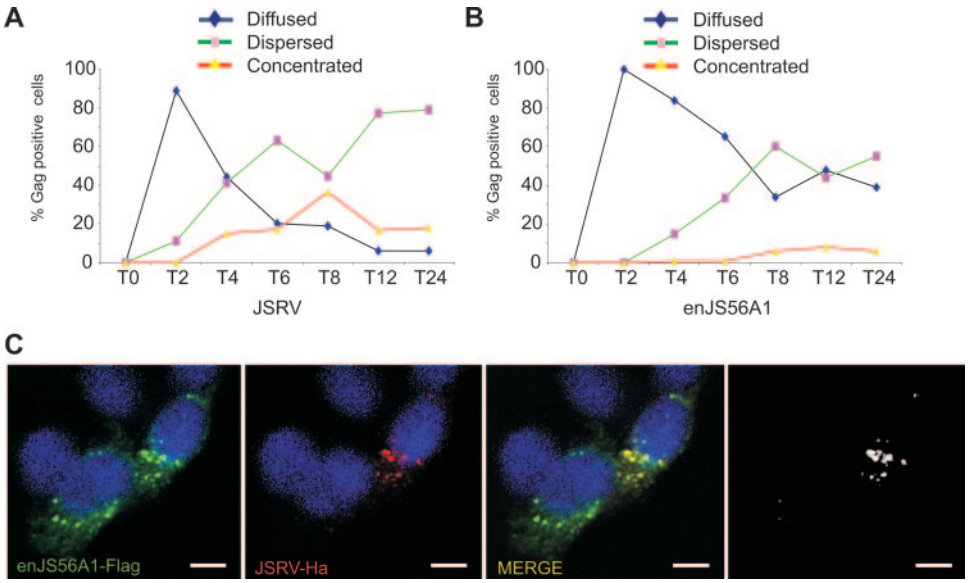

FIG. 1. Kinetics of JSRV/enJS56A1 Gag staining pattern. (A and B) Quantification of JSRV and enJS56A1 Gag staining pattern in confocal microscopy of HeLa cells at various time points posttransfection. The number of cells in which Gag accumulation was observed diffused, dispersed, and concentrated was counted. Approximately 100 cells were evaluated at each time point. Graphs represent the average of two independent experiments. (C) HeLa cells expressing JSRVHA-MA and enJS56A1Flag-MA were fixed at the 4-h time point and analyzed by confocal microscopy using antibodies to the Flag (green) and Ha (red) epitopes and appropriate secondary conjugated antibodies. Scale bars, 10 μm.

types were also evident, especially in cells displaying both diffused and dispersed pattern of staining (24). Cells expressing enJS56A1 Gag also show staining patterns similar to the ones described above, although in general the staining is more intense than in cells expressing JSRV Gag. In addition, concentrated Gag staining is localized at the MTOC in cells expressing JSRV but not in those expressing enJS56A1 (24).

In all our previous studies we analyzed cells 24 to 48 h after transfection by confocal microscopy. In order to better correlate the staining pattern observed with the kinetics of Gag intracellular trafficking, we analyzed cells transfected with JSRV or enJS56A1 expression plasmids at 3 h posttransfection (taken as time zero for these experiments) and at various time points up to 24 h (Fig. 1A and B).

No positive cells expressing JSRV or enJS56A1 were detected at time zero. Both cells expressing JSRV and enJS56A1 showed ~90% of the positive cells with a uniformly diffused Gag staining pattern after 2 h. Cells with a diffused phenotype decreased rapidly at later time points, although enJS56A1 reached a plateau of 30 to 40% of Gag-positive cells at 8 h. Conversely, we observed that the relative fraction of Gag-positive cells with a dispersed phenotype increased over time in both JSRV- and enJS56A1-expressing cells. We also noticed that the number of cells with a mixed diffused-dispersed Gag staining pattern increased with time. Consequently, we grouped these cells with the dispersed category since both groups showed the same kinetics in these assays.

The concentrated phenotype in JSRV-expressing cells increased in the first 8 h and then decreased slightly. Again, we found intermediate phenotypes at later time points especially in cells displaying both dispersed and concentrated phenotypes and here we counted as "concentrated" also cells with a "mixed" phenotype as far as concentrated Gag staining was clearly visible. The number of cells expressing enJS56A1 with a concentrated Gag staining pattern increased slowly with time but remained lower than the JSRV-expressing cells.

In a previous study we showed that JSRV and enJS56A1 Gag colocalize when coexpressed within the same cell (24). Here we extended our previous observations and determined that JSRV and enJS56A1 Gag colocalize at very early time points when cells with a dispersed phenotype begin to appear (4 h; Fig. 1C).

JSRV Gag myristoylation-defective mutant accumulates at the MTOC region. Previous studies have shown that a M-PMV mutant with a myristoylation-defective Gag assembles normally but does not reach the cell membrane (34). We have shown that similar to M-PMV, mutant JSRV-G2A (residue G2 in Gag is essential for myristoylation) is defective and does not exit the cell (24).

Here, we first established that JSRV-G2A Gag staining concentrates at the MTOC (Fig. 2A). Next, we determined the kinetics of JSRV-G2A (Fig. 2B). The relative number of cells expressing JSRV-G2A with a diffuse Gag staining pattern was basically identical to the one of JSRV-expressing cells. Cells with a dispersed phenotype increased at 4 h but remained more or less constant until 24 h. On the contrary to JSRV expressing cells, the number of cells expressing JSRV-G2A with a concentrated Gag staining pattern increased steadily over a 24 h period when they reached 60 to 70% of the total positive cells. Thus, myristoylation-defective Gag completes only part of the normal intracellular trafficking by reaching the MTOC and accumulating in this region. Therefore, JSRV-G2A can be a useful experimental tool to understand at which point of the replication cycle JLR occurs.

We introduced the R21W mutation into JSRV-G2A and determined that the resulting double mutant (JSRV-G2AR21W)

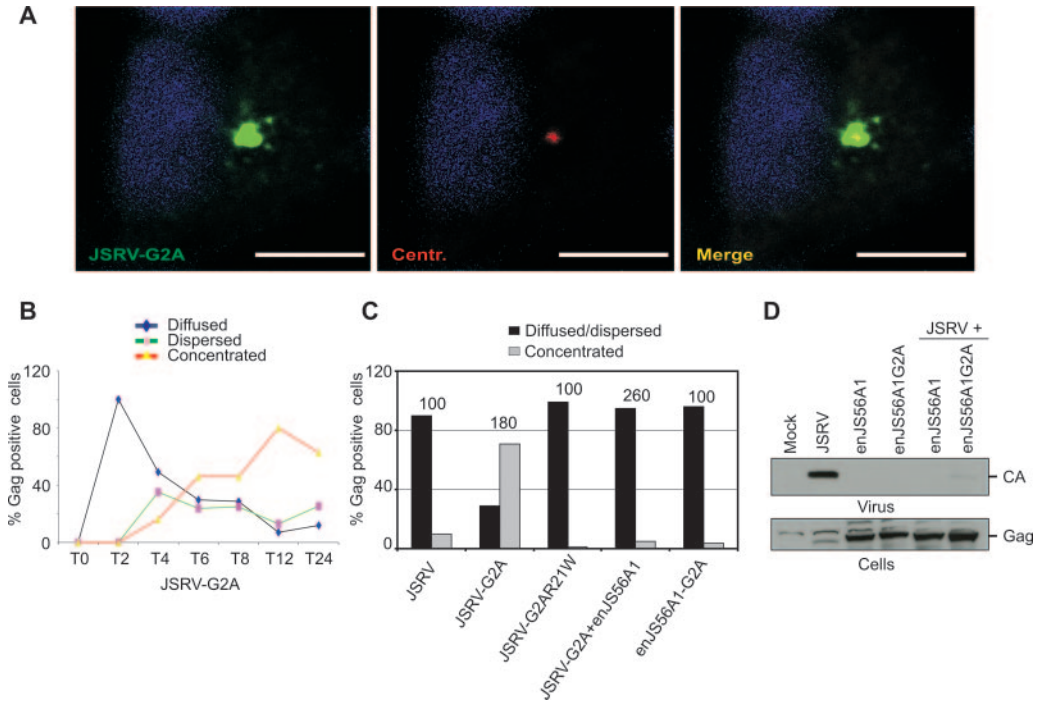

FIG. 2. Effects of myristoylation in Gag intracellular distribution and enJS56A1-induced restriction. (A) HeLa cells expressing JSRV-G2A were fixed at 24 h posttransfection and stained with anti-JSRV MA (green) and anti-γ-tubulin (red) antibodies. Scale bars, 10 μm. (B) Quantification of Gag staining patterns in confocal microscopy of HeLa cells expressing JSRV-G2A at various times posttransfection. Approximately 100 cells were evaluated at each time point. Graphs represent the average of two independent experiments. (C) Quantification of Gag staining pattern in JSRV and enJS56A1 myristoylation-defective mutants by confocal microscopy in HeLa cells at 24 h posttransfection. The graph represents the number of cells in which Gag staining was observed concentrated as opposed to diffused and dispersed. The number of cells counted in each experiment is represented on top of the bars. (D) SDS-PAGE and Western blotting of viral pellets (upper panel) and cell lysates (lower panel) of cells transfected with the indicated plasmids. Filters were incubated with antibodies to the JSRV CA.

did not accumulate at the MTOC, unlike the parental mutant JSRV-G2A. Thus, the transdominant phenotype conferred by the R21W mutation is dominant over Gag myristoylation and impairs JSRV Gag MTOC targeting (Fig. 2C). Most importantly, in cotransfection assays we determined that enJS56A1 blocks centrosome targeting of JSRV-G2A (Fig. 2C and D). Indeed, the relative number of cells expressing JSRV-G2A displaying a concentrated Gag staining is reduced more than 10 times in the presence of enJS56A1. In addition, an enJS56A1 myristoylation-defective mutant did not accumulate at the MTOC but was able to block JSRV exit as efficiently as wild-type enJS56A1, stressing the point that the myristoylation signal does not influence JLR (Fig. 2D).

Altogether, these data highlighted two postintegration events of JSRV Gag trafficking that can be described as "precentrosomal" and "postcentrosomal" depending on whether they take place before or after Gag reaches the MTOC. JLR occurs before JSRV Gag targets the MTOC.

JSRV Gag targeting of the MTOC requires dynein and an intact microtubule network. Microtubules direct intracellular organization by providing a dynamic structure in which motor proteins carry their cargo to specific compartments within the cell (9). Free movement of molecules with sizes over 20 nm is difficult within the cytoplasm (21). Given their size, intracellular Gag multimers and newly formed virions must use cellular motors to traffic within the cytoplasm (19) as, for example, suggested for M-PMV (38). We tested whether the microtubule network was required for JSRV and enJS56A1 Gag localization. To address this point, we first performed confocal microscopy on cells transfected with expression plasmids for the viruses indicated below and determined the staining pattern of Gag-expressing cells in the presence or absence of the microtubule-disrupting agent nocodazole. As shown in Fig. 3A, nocodazole induced a reduction in the relative number of cells with concentrated Gag staining in JSRV, JSRVHA-MA, and JSRV-G2A, whereas no effect was seen in cells expressing enJS56A1 or coexpressing JSRVHA-MA plus enJS56A1 (although the relative number of enJS56A1-expressing cells with a concentrated phenotype is very low even in the absence of nocodazole).

Altogether, our data indicate that JSRV Gag localization depends on intact microtubule network unless enJS56A1 is expressed within the same cell. Protein targeting toward the MTOC involves the dynein/dynactin motor protein complex (44). Dynein-dependent transport toward the minus end of microtubules can be specifically blocked by overexpression of dynamitin, the p50 subunit of dynactin (13). Expression of p50-GFP induced a drastic reduction of cells expressing JSRV or JSRV-G2A displaying a concentrated Gag phenotype (Fig. 3B). More importantly, overexpression of p50-GFP greatly reduced the release of JSRV viral particles (Fig. 3C), strongly suggesting that MTOC Gag targeting is an important step for JSRV to complete its replication cycle.

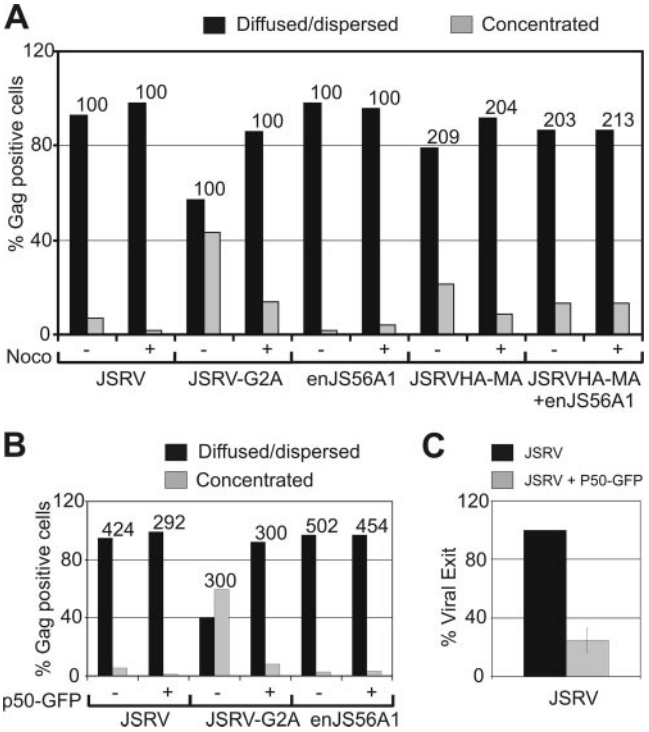

FIG. 3. The targeting of the JSRV Gag to the centrosomal region is dependent on dynein and intact microtubule network. (A) Quantification of JSRV, JSRV-G2A, enJS56A1, and JSRVHA-MA Gag staining patterns by confocal microscopy in HeLa cells after treatment with nocodazole or with the solvent dimethyl sulfoxide used as a negative control. Gag proteins were detected by using antibodies to JSRV MA or HA. The graph represents the number of cells in which Gag staining was observed concentrated as opposed to diffused or dispersed. The number of Gag-positive cells counted in each experiment is indicated above each bar. Note that the use of anti-HA antibodies, compared to polyclonal anti-JSRV-MA serum, results normally in a relatively higher percentage of cells with concentrated Gag staining and a lower percentage of cells displaying diffuse Gag. These differences are probably due to the different sensitivity of the two antisera. (B) The effect of p50-GFP on Gag staining pattern was evaluated as in panel A. The number of Gag-positive cells counted in each experiment is indicated above each bar. Note that only cells double positive for Gag and p50-GFP were counted. (C) Graph representing the quantification of three independent SDS-PAGE and Western blotting experiments of viral particles released in the supernatant of 293T cells transfected with a JSRV expression plasmid in the presence or absence of p50-GFP. Filters were incubated with an antiserum to the JSRV CA. Signals were quantified by chemifluorescence as described in Materials and Methods. Bars indicate the standard errors.

Trafficking of pericentriolar recycling endosomes is critical for JSRV exit. We next assessed the fate of JSRV Gag after reaching the MTOC. M-PMV Gag has been shown to colocalize with pericentriolar recycling endosomes (37). We wondered whether pericentriolar localization of JSRV Gag was a required step for this virus to exit exploiting the recycling endosome machinery. We detected in transiently transfected cells, by confocal microscopy, colocalization of the JSRV (and not enJS56A1) Gag with transferrin and Rab11 (Fig. 4). Transferrin is a general marker for recycling endosomes, while Rab11 is a small GTPase involved in pericentriolar recycling endosome trafficking and used as a specific marker for these organelles (22, 43).

JSRV Gag did not colocalize with any other cellular marker used in the present study, such as those for the endoplasmic reticulum, trans-Golgi bodies, late endosomes, lysosomes, processing bodies, and stress granules (data not shown). Minimal colocalization was found occasionally with early endosomes using antibodies to EEA1 (data not shown).

In order to assess the biological relevance of the data presented above, we tested whether the block of clathrin-dependent endocytosis by the GFP-tagged Eps15 dominant-negative mutant EΔ95/295 (1) affected virus exit. EΔ95/295 inhibited, as expected, endocytosis of fluorescence labeled transferrin, unlike the Eps-derived GFP fusion protein DIIIΔ2 that was used as a negative control (Fig. 5A). More importantly, EΔ95/295, and not DIIIΔ2, strongly inhibited JSRV exit in cotransfection assays (Fig. 5B).

These data indicate that vesicle trafficking is necessary for the efficient release of JSRV viral particles. Vesicle trafficking includes early endosomes, which traffic from the cell surface back to the plasma membrane in a fast recycling step, and a slow recycling pathway in which (recycling) endosomes traffic from the MTOC back to the cell surface. Rab11 is one of the major proteins involved in pericentriolar recycling endosome trafficking (43). Given the colocalization of JSRV Gag with Rab11, we assessed whether the slow recycling pathway was important for JSRV exit. To this end, we assessed JSRV exit in cells previously transfected with specific siRNAs for Rab11 or scrambled siRNAs. As shown Fig. 5C, Rab11 expression was efficiently decreased in all our experiments compared to control siRNAs. More importantly, JSRV exit was significantly decreased at 3, 6, and 12 h posttransfection in cells where Rab11 expression was almost completely blocked (Fig. 5C and D). However, other mechanisms that are Rab11 independent may be important for JSRV exit considering that Rab11 knockdown did not abrogate completely viral exit.

By confocal microscopy of JSRV-expressing cells we observed that both expression of EΔ95/295 and inhibition of Rab11 by siRNAs increased the relative number of cells with concentrated Gag in the MTOC region (data not shown). Thus, Gag trafficking toward the MTOC appears to be independent from vesicle trafficking since EΔ95/295 also blocks endosome trafficking toward the MTOC. This interpretation is supported by another set of experiments in which we inhibited endocytic and secretory pathways by incubating cells at 20°C. At this temperature, endocytosis and transport of transferrin from the cell surface to the MTOC are permitted, while recycling of the endosomes toward the cell membrane is disrupted (32). Cells expressing JSRV and incubated at 20°C displayed a fourfold increase of JSRV Gag accumulation to the MTOC (concentrated phenotype). On the other hand, enJS56A1 concentrated Gag localization within the cell was not affected by incubation at low temperatures (data not shown). These results suggest once again that JSRV and not enJS56A1 use the vesicular trafficking.

enJS56A1 Gag forms microaggregates developing into an aggresome in the presence of lactacystin. The results thus far have indicated that enJS56A1 and JSRV Gag localization and trafficking within the cell are different. By confocal microscopy,

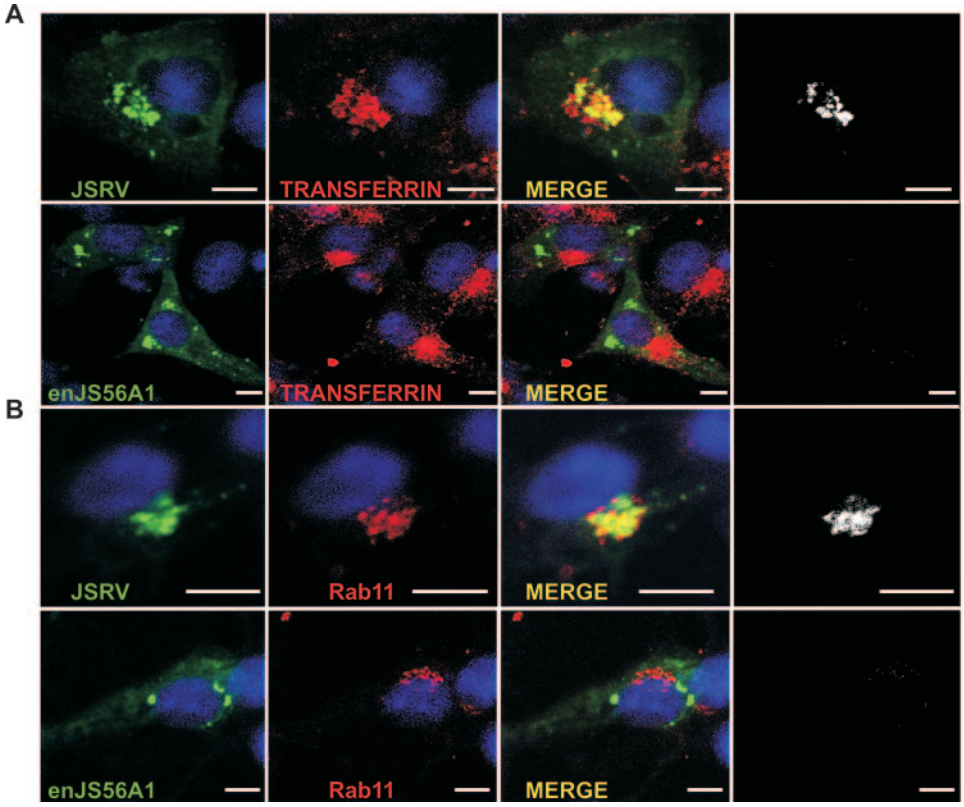

FIG. 4. JSRV Gag colocalizes with pericentriolar Rab11-positive endosomes. (A) HeLa cells were transfected with JSRV- or enJS56A1-expressing plasmids. At 24 h posttransfection, cells were transferred to serum-free medium for 1 h and incubated with fresh medium containing transferrin conjugated to Alexa Fluor 568 (red). After 30 min of incubation, the cells were fixed and analyzed by confocal microscopy using antibodies to the JSRV MA and a secondary antibody conjugated with Alexa Fluor 488. (B) HeLa cells transfected with JSRV or enJS56A1 expression plasmids were fixed and analyzed by confocal microscopy using antibodies to JSRV MA and Rab11a with the appropriate conjugates. Panels in black and white show colocalization using the plug-in of the Image J program. Scale bars, 10 μm.

we could not colocalize enJS56A1 Gag with any of the cellular organelle markers used, including those for the endoplasmic reticulum, trans-Golgi bodies, late endosomes, early endosomes, recycling endosomes, lysosomes, processing bodies, and stress granules (data not shown).

However, we observed extensive colocalization between enJS56A1 Gag and the aggresome marker GFP-250 in microaggregates dispersed throughout the cytoplasm. GFP-250 is a misfolded GFP protein that forms small aggregates dispersed within the cytoplasm before being transported to the MTOC. Reorganized intermediate filaments of vimentin normally surround aggresomes (14). enJS56A1 (but not JSRV) Gag colocalized with the dispersed microaggregates of GFP-250 proteins but not with the one accumulated at the MTOC (Fig. 6A). Microaggregates are usually formed by misfolded or unfolded proteins that can be polyubiquitinylated (14). Indeed, enJS56A1 Gag colocalized with polyubiquitinylated proteins using an antibody against polyubiquitin residues (Fk1) (Fig. 6B).

The data shown above suggest that enJS56A1 Gag forms microaggregates, dispersed in the cytoplasm, that do not progress to form a proper aggresome. The most likely explanation for this phenomenon is that enJS56A1 Gag (in the presence or absence of JSRV Gag) is degraded by the proteasome machinery and never reaches the threshold necessary to induce the formation of aggresomes. Indeed, in the presence of the proteasome inhibitor lactacystin, enJS56A1 (but not JSRV) Gag accumulated at the MTOC in a microtubule-dependent manner and colocalized with GFP-250 in this area (Fig. 7A and B). Negative controls included cells treated with EtOH, which was used to solubilize lactacystin. Cells with enJS56A1 concentrated at the MTOC display vimentin reorganization typical of aggresomes (Fig. 7C). We observed, by Western blotting of lysates of cells expressing enJS56A1 and treated with lactacystin, an increase of the cleaved ("mature") Gag compared to control untreated cells (Fig. 7D). In addition, longer exposures of Western blots revealed small amounts of viral particles in the supernatants of enJS56A1 cells treated with lactacystin. Thus, enJS56A1 can form (at least partially) viral particles considering that cleavage of the immature Gag precursor can occur only upon assembly. These data are in agreement with our previous observations of enJS56A1 viral particles by electron microscopy (23). JLR is not abrogated by lactacystin, indicating that proteasomal degradation is necessary to eliminate excess Gag from the cells but is not per se the cause of restriction (data not shown). Thus, enJS56A1 Gag disrupts JSRV Gag trafficking by sequestering it into microaggregates that are then likely degraded by the proteasome machinery.

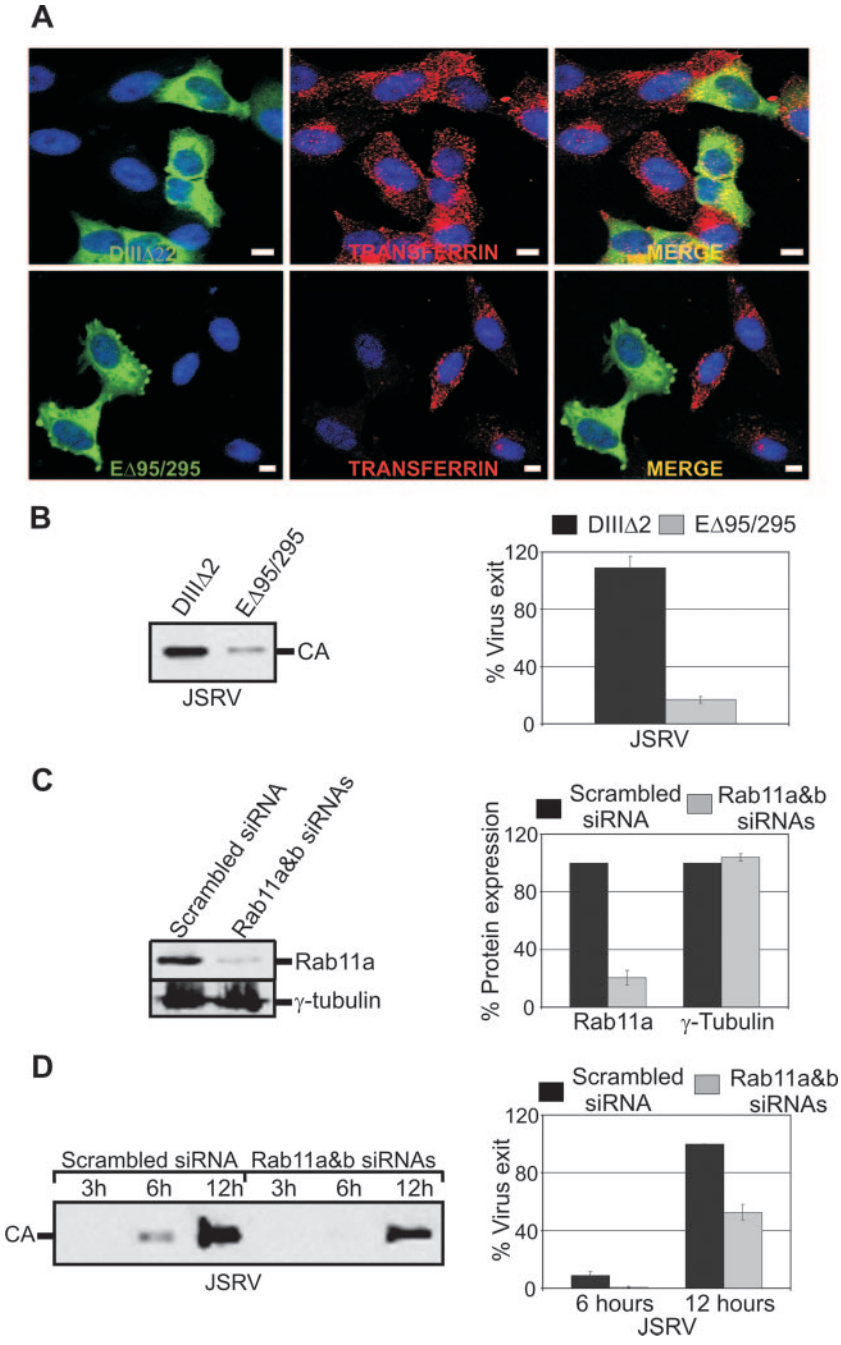

FIG. 5. JSRV exit from the cells is facilitated by functional recycling endosomes. (A) HeLa cells were transfected with plasmids expressing the GFP-tagged DIIIΔ2 or EΔ95/295. At 24 h posttransfection, cells were transferred to serum-free medium for 1 h. Cells were then washed and incubated in fresh medium containing transferrin conjugated to Alexa Fluor 568 (Red). After 30 min of incubation, cells were fixed and images acquired. Scale bars, 10 μm. (B) Western blot analysis of JSRV in presence of DΔ2 or EΔ95/295. Viral pellets of cells transfected with the indicated plasmids were resolved by SDS-PAGE and immunoblotted with an antiserum to JSRV CA. The graph shows the quantification by chemifluorescence of three independent Western blotting experiments as described in Materials and Methods. (C) Western blot analysis of Rab11 expression after siRNA treatment. Lysates of cells transfected with a scrambled siRNA or Rab11a and Rab11b siRNAs were resolved by SDS-PAGE and immunoblotted with antibodies to Rab11a (upper panel) or γ-tubulin (lower panel). Three independent experiments were quantified as in panel B. (D) Western blot analysis of JSRV viral particles release in cells treated with the indicated siRNAs using antibodies to the JSRV CA. The graph shows the quantification of signal intensities given by the virus pellets in three independent experiments as described in Materials and Methods (bars indicate the standard errors).

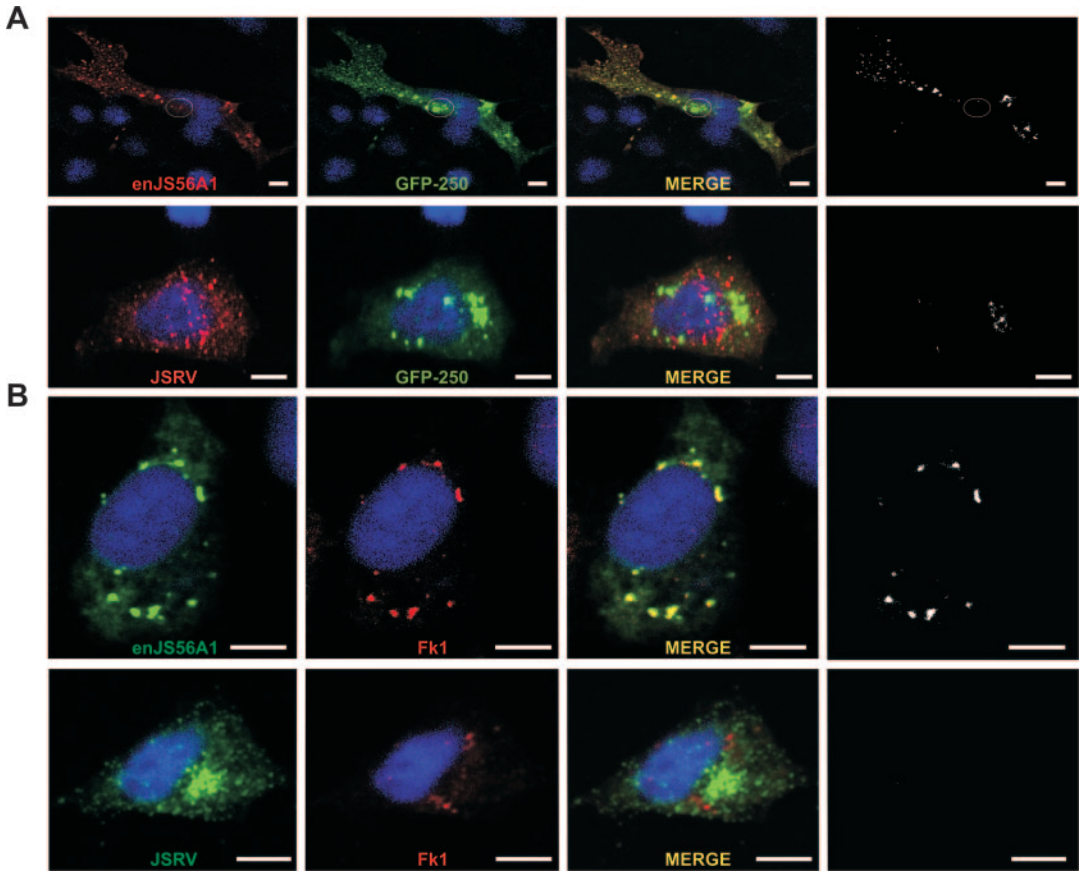

FIG. 6. enJS56A1 Gag colocalizes with GFP-250 and polyubiquitin-rich residues. (A) HeLa cells were cotransfected with plasmids expressing either enJS56A1 or JSRV with the aggresome marker GFP-250. At 24 h after transfection, cells were fixed and analyzed by confocal microscopy using an antiserum to the JSRV MA and the appropriate conjugate. Black and white pictures showing colocalization were obtained with the Image J program. (B) HeLa cells were transfected with JSRV- or enJS56A1-expressing plasmids. At 24 h after transfection, cells were fixed and analyzed by confocal microscopy using antibodies to the JSRV MA and polyubiquitin residues (Fk1) with the appropriate fluorescent conjugates. Black and white pictures showing colocalization were obtained with the Image J program. Scale bars, 10 μm.

DISCUSSION

In this study, we have investigated the mechanisms of JSRV late restriction. Our data show that enJS56A1 blocks JSRV by inhibiting Gag trafficking to the pericentriolar/MTOC area. enJS56A1 Gag accumulates in microaggregates that colocalize with GFP-250, an aggresome marker. However, the colocalization between enJS56A1 Gag and GFP-250 occurs only in dispersed areas throughout the cytoplasm and not within an aggresome at the MTOC, unless the proteasomal machinery is inhibited by lactacystin.

Thus, enJS56A1 Gag displays properties of misfolded proteins forming aggregates dispersed in the cell, which are subsequently degraded by the proteasome. During folding, proteins exposing hydrophobic domains or residues can lead to the formation of aggregates (46). The substitution of an arginine residue in the JSRV Gag at position 21 with the highly hydrophobic tryptophan in enJS56A1 might alter the overall surface conformation of Gag resulting in multimers and/or particles that cannot traffic and are subsequently degraded by the proteasome. However, inhibition of the proteasomal machinery did not allow JSRV exit in the presence of enJS56A1, indicating that JLR is due to the inability of Gag to traffic properly within the cytoplasm rather than the targeting of the proteasome per se. In vivo, a tight balance between enJS56A1 Gag synthesis, aggregation and proteasome degradation might be important since accumulation of aggregates may be toxic for the cell.

The degradation of enJS56A1 Gag by the proteasome is reminiscent of the action of Trim5α, a cellular restriction factor (20). Trim5α blocks retroviruses at postentry steps, but it has been shown recently that it can also induce Gag degradation during late phases of the replication cycle (36). Trim5α can accumulate in cytoplasmic bodies that form an aggresome in the presence of proteasome inhibitors (47). The functional properties of these cytoplasmic bodies are not completely clear; nevertheless, they are highly dynamic structures moving along the microtubule network (7, 30). From our studies, it appears that enJS56A1 Gag localization is not dependent on the microtubule network/dynein. However, we cannot rule out the possibility that enJS56A1 Gag aggregates are dynamic rather than a dead-end structure. Live fluorescence microscopy would address this issue, but thus far we have not been able to obtain functional JSRV/enJS56A1 Gag-GFP fusion proteins.

Interestingly, expression of the C-terminal half of the ESCRT

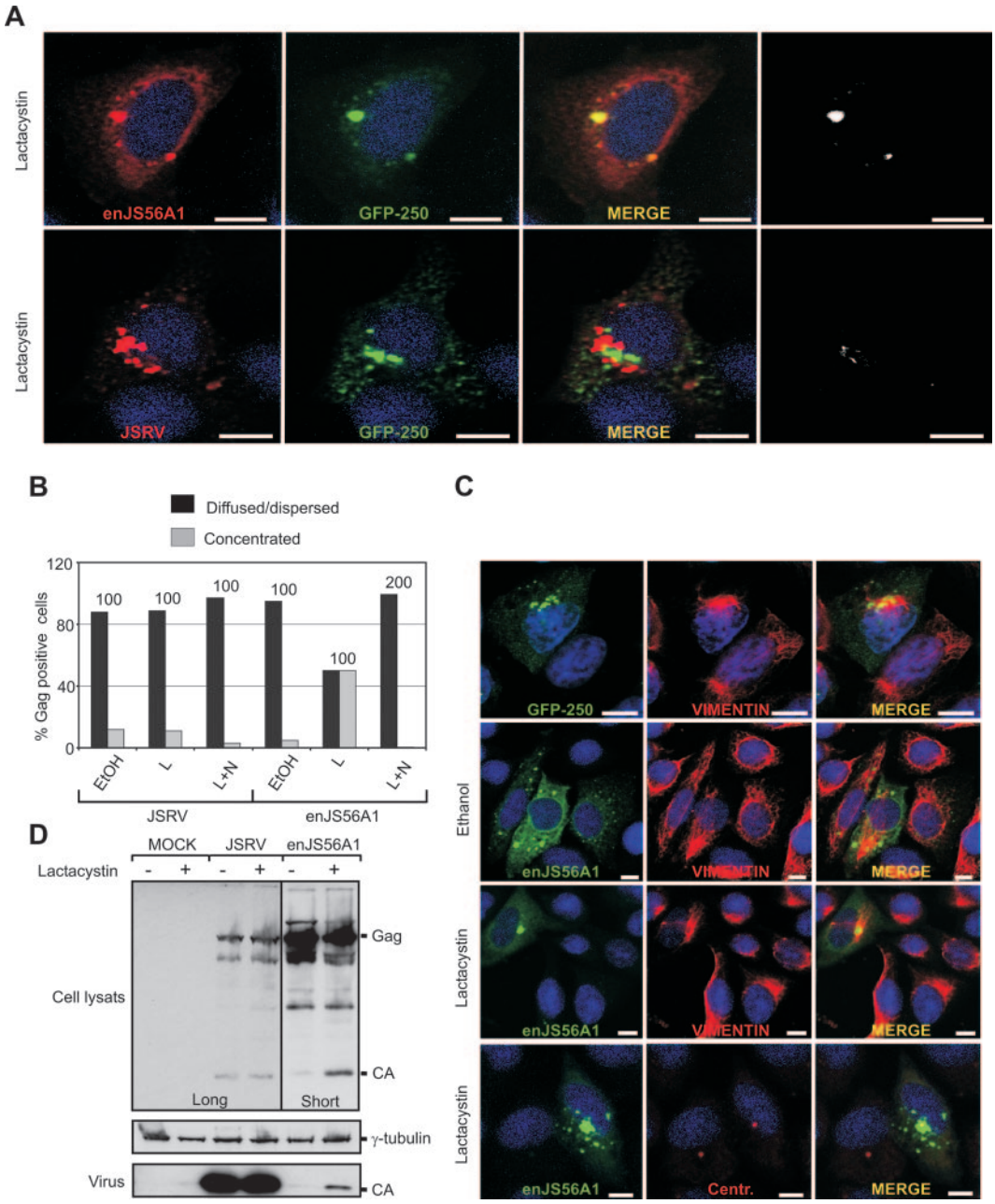

FIG. 7. enJS56A1 Gag forms an aggresome in the presence of lactacystin. (A) HeLa cells were cotransfected with GFP-250 and either JSRV or enJS56A1 expression plasmids. At 24 h posttransfection cells were treated with lactacystin for 6 h and then fixed and analyzed by confocal microscopy using an antiserum to JSRV MA with the appropriate labeled secondary antibody. Colocalization between enJS56A1 Gag and GFP-250 is shown also in black and white images obtained with the plug-in of the Image J program. (B) Quantification of JSRV and enJS56A1 Gag staining patterns by confocal microscopy in HeLa cells after treatment with lactacystin (6 h) (L), lactacystin plus nocodazole (L+N) for 4 h, or EtOH. EtOH was used as a solvent for lactacystin and was also used as a negative control. Gag was detected by using antibodies to JSRV MA and the appropriate conjugate. The graph represents the number of cells in which Gag staining was observed concentrated as opposed to diffused and dispersed. The number of Gag-positive cells counted in each experiment is indicated above each bar. (C) HeLa cells were transfected with plasmids expressing GFP-250 or enJS56A1. At 24 h after transfection, some of the cells (as indicated) were treated with lactacystin or ethanol as a negative control for further 12 h. Cells were then fixed and analyzed by confocal microscopy using antibodies to vimentin antibody labeled with Cy3 (Red), γ-tubulin, or JSRV Gag in the presence of appropriate secondary antibodies. Scale bars, 10 μm. (D) SDS-PAGE and Western blotting analysis of cells expressing JSRV and enJS56A1 in the presence or absence of lactacystin. Two different exposures of the same gel (indicated as "Long" and "Short") are shown in the figure to better appreciate the different levels of Gag in the presence or absence of lactacystin. Filters were incubated with antibodies to the JSRV CA or γ-tubulin to control for loading uniformity.

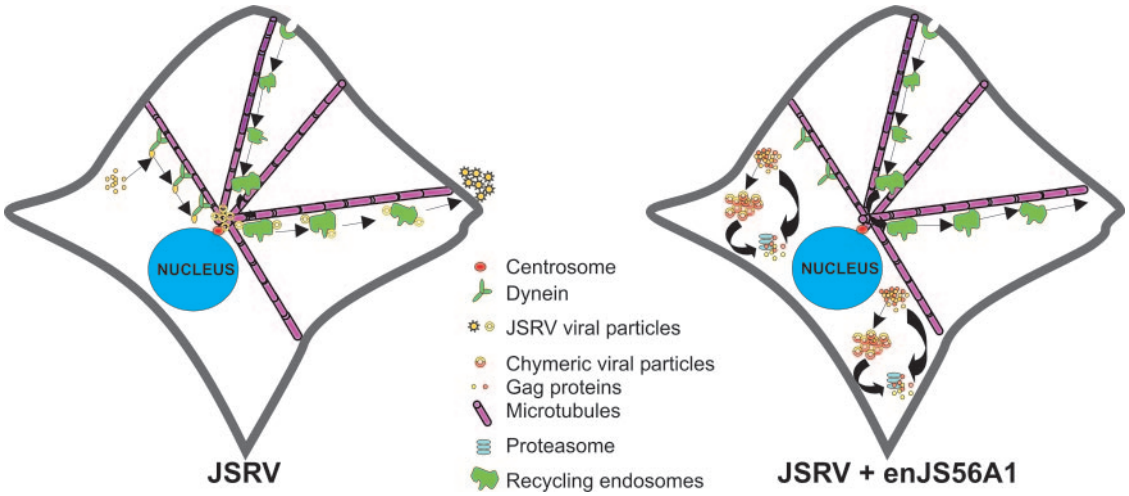

FIG. 8. Model of JSRV Gag trafficking and enJS56A1 restriction. See Discussion for details.

I protein TSG101 induces sequestration of Rous sarcoma virus Gag into intracellular structures that colocalize with GFP-250 and are enriched in ubiquitin but do not form proper aggresomes (16). Thus, it appears that retroviral Gag trafficking can be efficiently blocked by different proteins resulting in similar outcomes.

We have arbitrarily divided the posttranslational mechanisms of JSRV replication into "precentrosomal" and "postcentrosomal." JSRV Gag is targeted to the MTOC by a process dependent on dynein and an intact microtubule network. We speculate that JSRV Gag multimerizes before MTOC targeting, given that we observed the presence of dispersed dots of Gag staining in the cytoplasm by confocal microscopy, before the appearance of concentrated Gag at the MTOC. Once Gag reaches the MTOC, it needs an intact endocytic pathway and slow recycling endosomes trafficking to exit efficiently from the cell (Fig. 8). We speculate that the myristoyl group of JSRV Gag needs to interact with the membranes of the recycling endosomes (rather than the cell membrane such as in retroviruses with a type-C assembly) in order for the virus to exit efficiently. Indeed, we observed that myristoylation-defective Gag is defective for virus exit and accumulates at the MTOC area.

Some betaretroviruses, such as M-PMV, possess an 18-amino-acid sequence within the MA domain, known as the cytoplasmic targeting/retention signal (CTRS), that is a dominant signal for intracytoplasmic assembly of immature capsids. A single arginine-to-tryptophan substitution in position 55 of the CTRS abrogates its dominant activity and allows M-PMV to follow a C-type morphogenic pathway (33, 35). Conversely, insertion of the CTRS of M-PMV into the murine leukemia virus results in intracytoplasmic assembly of an otherwise type C retrovirus (8). Previous work has shown that the subcellular site of M-PMV assembly is the pericentriolar region. Gag MTOC targeting occurs cotranslationally via dynein-mediated transport, is determined by the CTRS, and depends on intact microtubules (37, 38). Our results suggest that the R21W mutation in enJS56A1 Gag does more than just disrupt a CTRS-like function because enJS56A1 does not exit the cells at all. However, overall, the data presented in this study suggest that JSRV and M-PMV have remarkably similar morphogenesis and intracellular trafficking pathways (37, 38).

Unfortunately, JSRV does not grow in tissue culture, and our assays have to be performed in transfected cells. Transient transfections could lead in some cases to misleading results if proteins are overexpressed. However, in our case, enJS56A1 blocks JSRV exit despite overexpression of the latter. Indeed, we have shown that enJS56A1 can still block JSRV when expression plasmids driven by the same promoter are transfected at a ratio of 1 (for enJS56A1) to 10 (for JSRV) (23). In addition, in the same assays, an enJS56A1 mutant with a deletion in the major homology region (required for retroviral assembly) of the CA did not interfere with JSRV (23, 24). Furthermore, dominant-negative properties to JSRV are conferred only by mutations of the arginine residue in position 21 in Gag such as the R21W substitution present in enJS56A1 (23, 24). For example, JSRV L- or M-domain mutants are defective for virus exit but are not transdominant in our assays (23, 24).

Finally, we have recently discovered in the sheep genome a second provirus (enJSRV-20) with the same transdominant properties of enJS56A1. The critical R21W substitution in Gag for both enJS56A1 and enJSRV-20 has been acquired during evolution in two temporally distinct events (which are now fixed in the domestic sheep) suggestive of positive selection. Importantly, we have discovered the occurrence of newly integrated proviruses escaping JLR, suggesting that this mechanism of viral evolution is shaping the coevolution of sheep and sheep betaretroviruses (Arnaud, unpublished).

ACKNOWLEDGMENTS

We thank A. Benmerah, E. S. Sztul, and R. B. Vallee for reagents and A. Saib, L. Scobie, G. W. Gould, M. Varela, and members of the Laboratory of Viral Pathogenesis for invaluable advice.

This study was funded by a program grant from the Wellcome Trust. M.P. is a Wolfson-Royal Society research merit awardee.

REFERENCES

1. **Benmerah, A., M. Bayrou, N. Cerf-Bensussan, and A. Dautry-Varsat.** 1999. Inhibition of clathrin-coated pit assembly by an Eps15 mutant. J. Cell Sci. **112**(Pt. 9)**:**1303–1311.
2. **Best, S., P. Le Tissier, G. Towers, and J. P. Stoye.** 1996. Positional cloning of the mouse retrovirus restriction gene Fv1. Nature **382:**826–829.

3. **Best, S., P. R. Le Tissier, and J. P. Stoye.** 1997. Endogenous retroviruses and the evolution of resistance to retroviral infection. Trends Microbiol. **5:**313–318.
4. **Bieniasz, P. D.** 2004. Intrinsic immunity: a front-line defense against viral attack. Nat. Immunol. **5:**1109–1115.
5. **Bieniasz, P. D.** 2003. Restriction factors: a defense against retroviral infection. Trends Microbiol. **11:**286–291.
6. **Boeke, J. D., and J. P. Stoye.** 1997. Retrotransposons, endogenous retroviruses and the evolution of retroelements, p. 343–436. *In* J. M. Coffin, S. H. Hughes, and H. E. Varmus (ed.), Retroviruses. Cold Spring Harbor Laboratory Press, Plainview, NY.
7. **Campbell, E. M., M. P. Dodding, M. W. Yap, X. Wu, S. Gallois-Montbrun, M. H. Malim, J. P. Stoye, and T. J. Hope.** 2007. TRIM5α cytoplasmic bodies are highly dynamic structures. Mol. Biol. Cell **18:**2102–2111.
8. **Choi, G., S. Park, B. Choi, S. Hong, J. Lee, E. Hunter, and S. S. Rhee.** 1999. Identification of a cytoplasmic targeting/retention signal in a retroviral Gag polyprotein. J. Virol. **73:**5431–5437.
9. **Dammermann, A., A. Desai, and K. Oegema.** 2003. The minus end in sight. Curr. Biol. **13:**R614–R624.
10. **DeMartini, J. C., J. O. Carlson, C. Leroux, T. Spencer, and M. Palmarini.** 2003. Endogenous retroviruses related to jaagsiekte sheep retrovirus. Curr. Top. Microbiol. Immunol. **275:**117–137.
11. **Dunlap, K. A., M. Palmarini, and T. E. Spencer.** 2006. Ovine endogenous betaretroviruses (enJSRVs) and placental morphogenesis. Placenta **2006**(Suppl. A)**:**S135–S140.
12. **Dunlap, K. A., M. Palmarini, M. Varela, R. C. Burghardt, K. Hayashy, J. L. Farmer, and T. E. Spencer.** 2006. Endogenous retroviruses regulate periimplantation conceptus growth and differentiation. Proc. Natl. Acad. Sci. USA **103:**14390–14395.
13. **Echeverri, C. J., B. M. Paschal, K. T. Vaughan, and R. B. Vallee.** 1996. Molecular characterization of the 50-kD subunit of dynactin reveals function for the complex in chromosome alignment and spindle organization during mitosis. J. Cell Biol. **132:**617–633.
14. **Garcia-Mata, R., Z. Bebok, E. J. Sorscher, and E. S. Sztul.** 1999. Characterization and dynamics of aggresome formation by a cytosolic GFP-chimera. J. Cell Biol. **146:**1239–1254.
15. **Hatziioannou, T., D. Perez-Caballero, A. Yang, S. Cowan, and P. D. Bieniasz.** 2004. Retrovirus resistance factors Ref1 and Lv1 are species-specific variants of TRIM5α. Proc. Natl. Acad. Sci. USA **101:**10774–10779.
16. **Johnson, M. C., J. L. Spidel, D. Ako-Adjei, J. W. Wills, and V. M. Vogt.** 2005. The C-terminal half of TSG101 blocks Rous sarcoma virus budding and sequesters Gag into unique nonendosomal structures. J. Virol. **79:**3775–3786.
17. **Jouvenet, N., S. J. Neil, C. Bess, M. C. Johnson, C. A. Virgen, S. M. Simon, and P. D. Bieniasz.** 2006. Plasma membrane is the site of productive HIV-1 particle assembly. PLoS Biol. **4:**e435.
18. **Keckesova, Z., L. M. Ylinen, and G. J. Towers.** 2004. The human and African green monkey TRIM5alpha genes encode Ref1 and Lv1 retroviral restriction factor activities. Proc. Natl. Acad. Sci. USA **101:**10780–10785.
19. **Leopold, P. L., and K. K. Pfister.** 2006. Viral strategies for intracellular trafficking: motors and microtubules. Traffic **7:**516–523.
20. **Luban, J.** 2007. Cyclophilin A, TRIM5, and resistance to human immunodeficiency virus type 1 infection. J. Virol. **81:**1054–1061.
21. **Luby-Phelps, K.** 2000. Cytoarchitecture and physical properties of cytoplasm: volume, viscosity, diffusion, intracellular surface area. Int. Rev. Cytol. **192:**189–221.
22. **Mohrmann, K., and P. van der Sluijs.** 1999. Regulation of membrane transport through the endocytic pathway by rabGTPases. Mol. Membr. Biol. **16:**81–87.
23. **Mura, M., P. Murcia, M. Caporale, T. E. Spencer, K. Nagashima, A. Rein, and M. Palmarini.** 2004. Late viral interference induced by transdominant Gag of an endogenous retrovirus. Proc. Natl. Acad. Sci. USA **101:**11117–11122.
24. **Murcia, P. R., F. Arnaud, and M. Palmarini.** 2007. The transdominant endogenous retrovirus enJS56A1 associates with and blocks intracellular trafficking of the JSRV Gag. J. Virol. **81:**1762–1772.
25. **Palmarini, M., and H. Fan.** 2001. Retrovirus-induced ovine pulmonary adenocarcinoma, an animal model for lung cancer. J. Natl. Cancer Inst. **93:**1603–1614.
26. **Palmarini, M., C. A. Gray, K. Carpenter, H. Fan, F. W. Bazer, and T. E. Spencer.** 2001. Expression of endogenous betaretroviruses in the ovine uterus: effects of neonatal age, estrous cycle, pregnancy, and progesterone. J. Virol. **75:**11319–11327.
27. **Palmarini, M., C. Hallwirth, D. York, C. Murgia, T. de Oliveira, T. Spencer, and H. Fan.** 2000. Molecular cloning and functional analysis of three type D endogenous retroviruses of sheep reveal a different cell tropism from that of the highly related exogenous jaagsiekte sheep retrovirus. J. Virol. **74:**8065–8076.
28. **Palmarini, M., M. Mura, and T. E. Spencer.** 2004. Endogenous betaretroviruses of sheep: teaching new lessons in retroviral interference and adaptation. J. Gen. Virol. **85:**1–13.
29. **Palmarini, M., J. M. Sharp, M. De las Heras, and H. Fan.** 1999. Jaagsiekte sheep retrovirus is necessary and sufficient to induce a contagious lung cancer in sheep. J. Virol. **73:**6964–6972.
30. **Perron, M. J., M. Stremlau, M. Lee, H. Javanbakht, B. Song, and J. Sodroski.** 2007. The human TRIM5alpha restriction factor mediates accelerated uncoating of the N-tropic murine leukemia virus capsid. J. Virol. **81:**2138–2148.
31. **Perron, M. J., M. Stremlau, B. Song, W. Ulm, R. C. Mulligan, and J. Sodroski.** 2004. TRIM5α mediates the postentry block to N-tropic murine leukemia viruses in human cells. Proc. Natl. Acad. Sci. USA **101:**11827–11832.
32. **Punnonen, E. L., K. Ryhanen, and V. S. Marjomaki.** 1998. At reduced temperature, endocytic membrane traffic is blocked in multivesicular carrier endosomes in rat cardiac myocytes. Eur. J. Cell Biol. **75:**344–352.
33. **Rhee, S. S., H. X. Hui, and E. Hunter.** 1990. Preassembled capsids of type D retroviruses contain a signal sufficient for targeting specifically to the plasma membrane. J. Virol. **64:**3844–3852.
34. **Rhee, S. S., and E. Hunter.** 1987. Myristylation is required for intracellular transport but not for assembly of D-type retrovirus capsids. J. Virol. **61:**1045–1053.
35. **Rhee, S. S., and E. Hunter.** 1990. Structural role of the matrix protein of type D retroviruses in Gag polyprotein stability and capsid assembly. J. Virol. **64:**4383–4389.
36. **Sakuma, R., J. A. Noser, S. Ohmine, and Y. Ikeda.** 2007. Rhesus monkey TRIM5α restricts HIV-1 production through rapid degradation of viral Gag polyproteins. Nat. Med. **13:**631–635.
37. **Sfakianos, J. N., and E. Hunter.** 2003. M-PMV capsid transport is mediated by Env/Gag interactions at the pericentriolar recycling endosome. Traffic **4:**671–680.
38. **Sfakianos, J. N., R. A. LaCasse, and E. Hunter.** 2003. The M-PMV cytoplasmic targeting-retention signal directs nascent Gag polypeptides to a pericentriolar region of the cell. Traffic **4:**660–670.
39. **Sheehy, A. M., N. C. Gaddis, J. D. Choi, and M. H. Malim.** 2002. Isolation of a human gene that inhibits HIV-1 infection and is suppressed by the viral Vif protein. Nature **418:**646–650.
40. **Spencer, T. E., M. Mura, C. A. Gray, P. J. Griebel, and M. Palmarini.** 2003. Receptor usage and fetal expression of ovine endogenous betaretroviruses: implications for coevolution of endogenous and exogenous retroviruses. J. Virol. **77:**749–753.
41. **Suzuki, S.** 1975. FV-4: a new gene affecting the splenomegaly induction by Friend leukemia virus. Jpn. J. Exp. Med. **45:**473–478.
42. **Swanstrom, R., and J. W. Wills.** 1997. Synthesis, assembly, and processing of viral proteins, p. 263–364. *In* J. M. Coffin, S. H. Hughes, and H. E. Varmus (ed.), Retroviruses. Cold Spring Harbor Laboratory Press, New York, NY.
43. **Ullrich, O., S. Reinsch, S. Urbe, M. Zerial, and R. G. Parton.** 1996. Rab11 regulates recycling through the pericentriolar recycling endosome. J. Cell Biol. **135:**913–924.
44. **Vallee, R. B., and M. P. Sheetz.** 1996. Targeting of motor proteins. Science **271:**1539–1544.
45. **Varela, M., Y. H. Chow, C. Sturkie, P. Murcia, and M. Palmarini.** 2006. Association of RON tyrosine kinase with the Jaagsiekte sheep retrovirus envelope glycoprotein. Virology **350:**347–357.
46. **Wetzel, R.** 1994. Mutations and off-pathway aggregation of proteins. Trends Biotechnol. **12:**193–198.
47. **Wu, X., J. L. Anderson, E. M. Campbell, A. M. Joseph, and T. J. Hope.** 2006. Proteasome inhibitors uncouple rhesus TRIM5α restriction of HIV-1 reverse transcription and infection. Proc. Natl. Acad. Sci. USA **103:**7465–7470.
48. **Yap, M. W., S. Nisole, C. Lynch, and J. P. Stoye.** 2004. Trim5α protein restricts both HIV-1 and murine leukemia virus. Proc. Natl. Acad. Sci. USA **101:**10786–10791.